applied sciences

MDPI

*Article*

# Highly Active under VIS Light M/$TiO_2$ Photocatalysts Prepared by Single-Step Synthesis

**Olga Thoda [1], Anastasia M. Moschovi [1,2], Konstantinos Miltiadis Sakkas [2], Ekaterini Polyzou [1] and Iakovos Yakoumis [1,2,*]**

[1] Monolithos Catalysts & Recycling Ltd., 83 Vrilissou, 11476 Athens, Greece
[2] YS Cypriot Catalysts Ltd., Lefkosias Avenue 50, Psevdas, Limassol 7649, Cyprus
* Correspondence: yakoumis@monolithos-catalysts.gr; Tel.: +30-2-106-450-106

**Abstract:** A single-step impregnation approach is investigated as a synthetic route for photocatalyst synthesis active under visible light. The as-derived photocatalysts exhibited very high degradation rates towards methylene blue (MB) decolorization under visible light despite the high concentration of the initial MB solution concentration. The $TiO_2$-based photocatalysts were prepared using nitrate precursor compounds for copper and silver; thus, Ag/$TiO_2$ and Cu/$TiO_2$ photocatalysts were prepared. The photocatalyst's physicochemical properties were determined by XRF, BET, and XRD analysis. The metal nature of the titania substrate, the titania matrix effect, and the metal concentration parameters were studied, while the catalyst concentration in the MB initial solution was optimized.

**Keywords:** photocatalyst; copper; silver; titania; rutile; anatase; visible light; photocatalysis; wet impregnation



**Citation:** Thoda, O.; Moschovi, A.M.; Sakkas, K.M.; Polyzou, E.; Yakoumis, I. Highly Active under VIS Light M/$TiO_2$ Photocatalysts Prepared by Single-Step Synthesis. *Appl. Sci.* **2023**, *13*, 6858. https://doi.org/10.3390/app13116858

Academic Editors: Petr Korusenko, Sergey Nesov and Raffaele Marotta

Received: 28 February 2023
Revised: 30 May 2023
Accepted: 31 May 2023
Published: 5 June 2023



## 1. Introduction

Methylene blue (MB) is an organic compound that is known as a significant water pollutant, contributing to the deterioration of the quality of water in oceans, seas, lakes, rivers, etc. It is a toxic and non-degradable chemical that is discharged from the textile industry. The photodegradation of MB is proven to be an effective method for pollutant removal, and it can be used to protect aquatic environments [1].

Methylene blue is also regarded as a benchmark substance for the performance testing of various photocatalysts. Methylene blue is a thiazine dye used in the textile industry, and it has regularly been exploited for comparing the effectiveness of synthesized photocatalysts by measuring the latter's ability to stimulate MB photodegradation. Titanium dioxide or titania ($TiO_2$) is an established photocatalyst with good capabilities concerning MB photodegradation; however, it is afflicted by a significant drawback: the limitation that restricts it to advantageously making use of the ultra-violet (UV) portion of solar radiation, which amounts to only 5% of solar radiation [2–5]. The adsorption–desorption equilibrium that is in effect during the degradation process when the catalyst is pure $TiO_2$ has been investigated, as well as the effects of the wavelength of the light in use, the concentration of $TiO_2$, and the initial MB concentration [5]. To remedy the aforementioned disadvantage of pure $TiO_2$ photocatalysts, various efforts have been made by using different metals, such as dopants, while also studying the effect of their concentration in the catalysts. The aim of experimenting with different doping agents is to facilitate the activation of the $TiO_2$ catalysts by visible light alongside UV radiation.

The role of the photocatalyst in the degradation of MB is absorbing light radiation, containing photons to enable electrons to migrate and create positively charged holes. These holes then cause the oxidation of water, forming hydroxyl radicals that target and degrade organic pollutants, such as MB [5].

In the literature, there have been several studied attempts at synthesizing photocatalysts for the degradation of methylene blue apart from using $TiO_2$, such as the doping

of ZnS nanoparticles with Cu under both visible and UV radiation [6]. The magnetite ($Fe_3O_4$)/$H_2O_2$ catalyst has also been studied under UV irradiation with the concentrations of magnetite, $H_2O_2$, and MB, as well as the initial pH and the source of light being parameters whose influence was evaluated through experimentation [7]. ZIF-8, a metal-organic framework (MOF), was studied on its use as a photocatalyst for the degradation of MB, and the effects of initial dye concentration and pH were considered [8]. Experimental studies with a $Co_3O_4$/ZnO nanocomposite prepared through precipitation have taken place in the literature for the evaluation of a photocatalyst for MB degradation [1]. A ZnO/Eu nanocomposite system has also been investigated as a possible catalyst for the degradation of MB [9]. A ZnO/$SnO_2$ nanocomposite has been reported in the literature as being able to boost the performance of pure ZnO [10].

On the other hand, the application of Co has been tested as a dopant for $TiO_2$ using a sol-gel method which exhibited better efficiency than pure $TiO_2$ under visible light; however, results were not equally promising for UV radiation [11]. Another case of $TiO_2$ doped with graphene has also been studied, aiming to create a porous composite that would be able to improve the degradation efficiency to a significant degree, as it exhibited a 6.5 times higher rate constant over Degussa P25 [12]. Furthermore, graphene oxide has been widely used as the precursor of graphene (GR) to synthesize graphite-based hybrid photocatalysts for solar-to-chemical energy conversion [13]. Au has been used to dope $TiO_2$ and has successfully improved its photocatalytic efficiency by almost 30% [14]. A V/Co/$TiO_2$ photocatalyst prepared by a sol-gel process has also been able to upgrade the degradation efficiency of $TiO_2$, as seen in the literature, by reducing the required irradiation time by 40% [15]. The use of Pt, as well as Au, have been investigated as possible dopants for $TiO_2$, with the positive result of a two-fold increase in the MB concentration that the photocatalysts can degrade in 1h of light exposure [16]. A nanocomposite Fe/$TiO_2$ photocatalyst has also been tested, while the performance of it revealed that the doped catalyst was able to perform better than pure $TiO_2$ due to a reduction in band gap energy of the Fe-$TiO_2$ composite to 1.45 eV [17]. The doping of $TiO_2$ with Ag, Sn, and Zn has been proven to enhance the photocatalytic efficiency of $TiO_2$ thin films, while Zn-doped $TiO_2$ films with a doping level of 5-mole percent exhibited the highest enhancement in photocatalytic properties [18]. On the other hand, the purity and nanostructure of the films are detrimental to efficient photocatalysis to suspend non-radiative recombination, according to numerous literature reports [19–21]. The addition of $MnTiO_3$ to $TiO_2$ has also been investigated in the literature and was found to be a good candidate for the removal of organic pollutants from industrial wastewater [22].

The addition of plasmonic metals (Au, Ag, and Cu) to $TiO_2$ has been researched, and the effect of pH on the photodegradation of MB has been documented. The improved photocatalytic performance observed is attributed to the altered electrical properties of the composite catalysts [23].

The study of the photocatalytic efficiency of Cu/$TiO_2$ nanocomposites, synthesized via atomic layer deposition (ALD), showed that the layer acted as a means of enhancing the photocatalytic activity of $TiO_2$ and the effect of the number of deposition cycles used was also investigated [24]. Another photocatalyst that has been studied in the literature is Cu/$TiO_2$ on $SiO_2$ substrate in order to facilitate nanoparticle formation. Nanoparticles were then studied to measure their efficiency in degrading MB when applied to building materials. The effect of Cu concentration on the catalyst performance was also studied, determining that there is an optimum level of doping (5 at.%) [25]. The use of $MoS_2$/Cu/$TiO_2$ nanoparticles prepared through hydrolysis has been investigated and exhibited improved performance compared to pure $TiO_2$. This is due to a decrease in the band gap values, their smaller crystallite size, the increase in the O adsorption, and the favoring of the anatase phase against rutile [26]. In the literature, the synthesis of Cu/$TiO_2$/MSM (mesoporous silica microsphere) has been studied, and the existence of an optimum concentration of Cu (0.1 wt%) has been documented [27]. The optimum concentration of copper could possibly depend on the structure and the properties of the matrix material, while the preparation

or deposition approach also affects and determines the properties of the composite materials. Thus, sol-gel methods report different optima in comparison with the sputtering methods [28,29].

Another metal that has recently been studied for potential employment as a doping agent in $TiO_2$ is Ag. A nanocomposite structure of $Ag/TiO_2$ synthesized via the use of plasma has been studied with respect to its property of activating the photodegradation of MB under solar light. An optimum amount of doping (2.0 mol.%) was observed, while it was also evidenced that Ag improved the photocatalytic properties of $TiO_2$ [30]. The synthesis of $Ag/TiO_2$ has also been studied when prepared through precipitation, and it resulted in an increase in the degradation efficiency in comparison to the pure $TiO_2$ catalyst. In the same study, the effect of Ag concentration was also determined through experimentation [31]. The catalytic behavior of thin $Ag/TiO_2$ films under UV light was the subject of a study whose conclusion was that the addition of Ag to the films leads to a significant improvement in the degradation efficiency versus a pure $TiO_2$ catalyst [32].

The use of Cu and Ag as co-dopants to $TiO_2$ substrate has been investigated, resulting in the observation that there is an optimum mixing ratio of doping metals (1 wt% Ag: 2 wt% Cu). The co-catalysts' photocatalytic degradation of MB and salicylic acid under visible irradiation was approximately 2–4 times higher than their monometallic counterparts, as the co-catalysts exhibited better synergistic effect, increased lifetime of the generated charge carriers, and active sites on the co-catalyst surface. The dual role of Ag and Cu metals resulted in enhanced photocatalytic performance in co-catalytic systems due to the combined functional behavior of deposited metals and improved interfacial charge transfer process [33]. Moreover, $Ni(OH)_2$-based co-catalysts have attracted increasing research interest in the field of solar-to-fuel conversion and, in particular, photocatalytic $H_2$ production and $CO_2$ reduction [34]. Last but not least, cobalt sulfide-based composites have also exhibited promising results in the field of solar fuel conversion and are being considered good candidates in photocatalytic hydrogen production, carbon dioxide reduction, nitrogen fixation, and photocatalytic degradation of pollutants due to their low cost and easy way of synthesis as well as their diverse structures [35].

Many efforts have been made to develop catalysts to improve the photocatalytic degradation of MB, indicating that they would be capable of being used on several other organic compounds to catalyze their photodegradation. Metals such as Cu and Ag have been focused on recently, with a variety of preparation techniques being studied. A common point in most of the performed research is that there is an optimum amount of dopant concentration, meaning that at first, the increase in the metal concentration has positive effects up to a certain amount that has been added, while the excess amount of metal in the catalyst negatively impacts the photodegradation efficiency of the catalyst.

Taking into consideration the studies that have been performed and the results that have been obtained by them, the current study aims to evaluate and optimize the single-step synthetic route for the preparation of $Cu/TiO_2$, $Ag/TiO_2$, and $Cu/Ag/TiO_2$ photocatalysts and assess their efficiency in degrading methylene blue dye. The importance of a single-step synthesis is rooted in its simplicity, as well as the time efficiency and cost-effectiveness, all of which are vital parameters regarding the sustainability of the method. The photocatalytic reaction took place at room temperature (25 °C) while targeting a relatively high initial MB concentration (250 ppm) for the lab-scale experiment. Furthermore, a parametric optimization of the materials was studied with respect to their effect on the photodegradation efficiency.

## 2. Materials and Methods

### *2.1. Catalyst Preparation*

The catalytic powder was prepared following the patented PROMETHEUS protocol described elsewhere [36,37].

All reagents used in this study for the preparation of Prometheus catalytic powder were commercial and were used without further purification. The chemical reagents

used were titanium (IV) oxide rutile (99.5% min metals basis, 1.0–2.0 Micron APS Powder, Alfa Aesar, Karlsruhe, Germany 43047), titanium (IV) oxide anatase (powder, 325 mesh, 99% Merck, Darmstadt, Germany), and ammonium hydroxide solution (Merck, percent concentration 25 wt%). As metal precursors, copper (II) nitrate trihydrate (Acros Organic, Geel, Belgium, purity 99%) or silver nitrate (ACS reagent, ≥99.0%) was added in solid form. The heterogeneous Prometheus catalyst was synthesized by the conventional wet impregnation method in various metal loadings and metal concentrations.

Mass calculations of materials used were performed to achieve the desired metal loading. Metal precursors were first dissolved in distilled water, and then titania support was added slowly under magnetic stirring. The pH was adjusted at 11 with 25% aq. $NH_4OH$, and the mixture was left at room temperature under magnetic stirring for 1h. Then, the solution was heated at 80–85 °C under continuous magnetic stirring. Most of the water was evaporated, and the resulting slurry was dried overnight in the beaker at 90 °C in a Binder drying furnace. After the completion of drying, the powder was collected from the beaker and placed in a muffle furnace for calcination at 500 °C for 1 h (heating ramp rate of 10 °C $min^{-1}$). Finally, the catalyst was received in powder form. A flowchart that depicts the experimental steps for the photocatalyst preparation is presented in Figure 1.

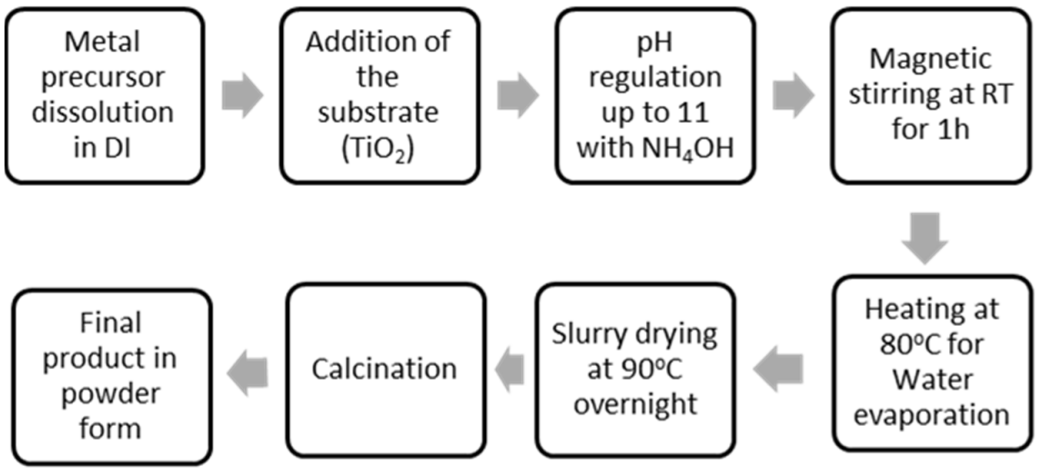


**Figure 1.** Experimental steps for the catalyst preparation.

*2.2. Characterization*

The crystal structure of commercial titanium dioxide substrates was determined with XRD (X-ray Diffraction) analysis using a Siemens D500 X-ray diffractometer. The crystalline phases of the prepared catalysts and the support material were determined by the XRD patterns. Data were collected for 2θ of 5° to 70° with step of 0.04°. The sample was measured in powder form, and its granulometry was under 250 μm.

Quantitative analysis was also performed with XRF (X-Ray Fluorescence Spectrophotometer) instrumentation (VANTA Olympus, 2017, Waltham, MA, USA). The calcined powder was grounded using a mortar and pestle set down to 250 μm. The granulometry was verified with a corresponding sieve of 250 μm.

The activity of the photocatalyst was assessed using a customized photocatalytic reactor. A double-jacketed 250 mL beaker, a magnetic stirrer, a Vis LED lamp (30 W E27, 230 V, wide beam 200°, cold white light 6200 k, light intensity 3500 lux Ra > 80, Pf > 0.5, and Energy class A+) with wavelength range 400–700 nm and a light shield box equipped with a fan for cooling the lamp, were used to perform the experiments, as shown in Figure 2. A double-beam UV-Vis spectrophotometer with a focal length of 190–1100 nm was used for the measurement of the light absorbance of the samples.

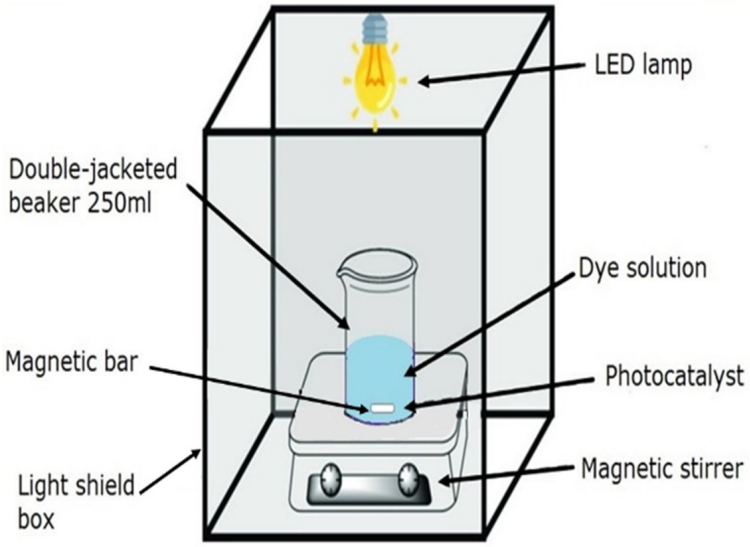


**Figure 2.** Schematic representation of customized photocatalytic reactor employed in the experimental procedure.

### *2.3. Photocatalytic Evaluation*

The photocatalytic efficiency of the prepared catalysts was evaluated towards the photocatalytic degradation of methylene blue ($C_{16}H_{18}N_3SCl{\cdot}3H_2O$, MB) using the self-prepared photocatalytic cell (Figure 3). The reaction progress was monitored by measuring the light absorbance of the MB solution with a UV-Vis spectrophotometer at 664 nm wavelength. For each measurement, 100 mL of MB aqueous solution with $C_o$ = 250 ppm was used as the target for the degradation. Then, a certain amount of catalyst was added to the MB aqueous solution, and the mixture remained in dark conditions for 30 min under stirring before being exposed to light radiation. The light absorbance of the reaction mixture reached equilibrium in almost 20 min under dark conditions. Therefore, 30 min of light shielding and stirring were enough for the mixture to reach adsorption−desorption equilibrium. Before sampling for the UV-Vis measurement, the mixture was left without stirring for 2 min. The collected samples were filtered through 0.45 μm CHROMAFIX XTRA discs to remove the remaining catalyst particles in the suspension to ensure the protection of the various chromatographic columns. A Beer–Lambert diagram was established to correlate the absorbance at 664 nm wavelength to MB concentration. The photocatalytic degradation of MB was conducted at room temperature.

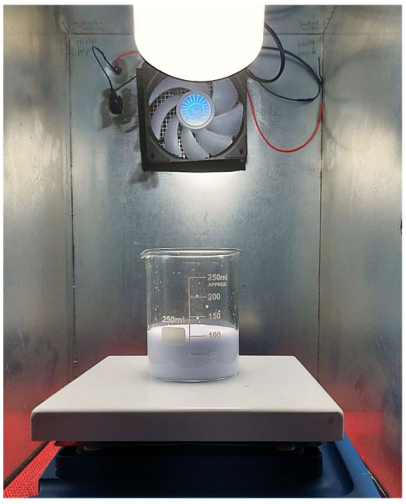

**Figure 3.** Picture of the photocatalytic reactor used in the experimental procedure.

## 3. Results and Discussion

### *3.1. X-ray Diffraction Analysis (XRD)*

The titania substrates were characterized by X-ray diffraction. The analysis was performed to establish the substrates' purity and verify their crystal form.

According to the XRD patterns of titania rutile and titania anatase (Figure 4), there were no reflections that have not been identified, indicating there were no impurities or unidentified phases in both substrates [38]. The metal-doped catalysts were also analyzed by XRD but provided spectra identical to their corresponding substrate. This might be attributed to the low metal concentration of the examined photocatalysts, which is below the detection limit of the instrument (~3%).

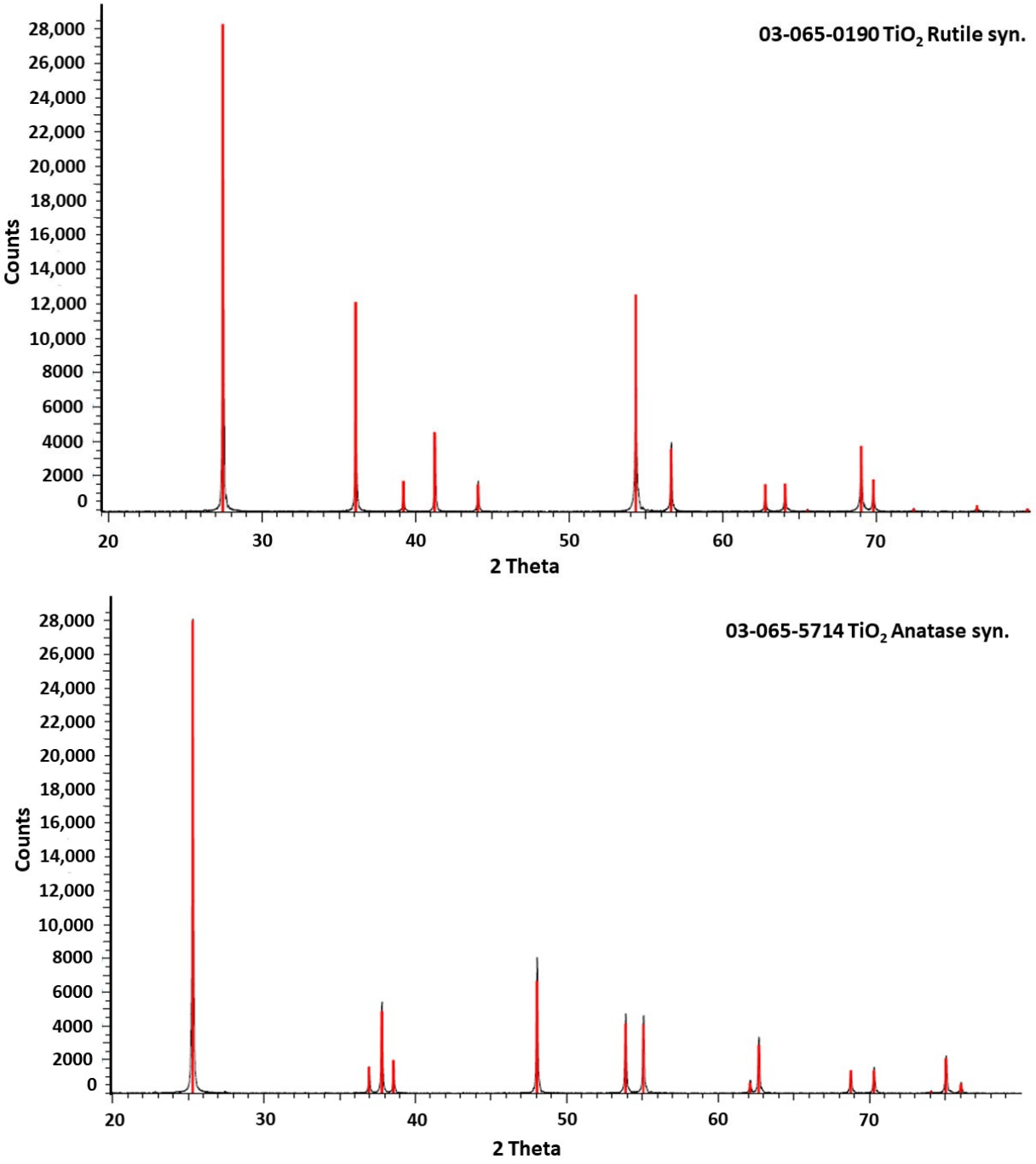


**Figure 4.** XRD analysis of employed substrates titania anatase and rutile.

### 3.2. X-ray Fluorescence Analysis (XRF)

The metal concentration on the titania substrate that was investigated was 0.1–1%, while commercially available titania rutile and anatase were employed in the photocatalyst preparation. Low metal loadings ranging between 0.1% and 1% were investigated. The metal loading on the $TiO_2$ support was determined by XRF analysis for each catalyst. The samples, their name, metal loading wt%, substrate composition, and metal composition determined by XRF spectrophotometry are listed in Table 1.

**Table 1.** List of as-prepared photocatalysts and their metal loading determined by XRF.

| Photocatalysts' Name | Metal | Metal Loading, wt% | Substrate Composition | Metal Concentration Determined by XRF, ppm |
|---|---|---|---|---|
| 0.1Cu/$TiO_2$ (R) | Cu | 0.1 | 100% Rutile | 998 |
| 0.25Cu/$TiO_2$ (R) | Cu | 0.25 | 100% Rutile | 2183 |
| 0.5Cu/$TiO_2$ (R) | Cu | 0.5 | 100% Rutile | 4012 |
| 1Cu/$TiO_2$ (R) | Cu | 1 | 100% Rutile | 8062 |
| 0.1Cu/$TiO_2$ (A) | Cu | 0.1 | 100% Anatase | 991 |
| 0.25Cu/$TiO_2$ (A) | Cu | 0.25 | 100% Anatase | 2216 |
| 0.5Cu/$TiO_2$ (A) | Cu | 0.5 | 100% Anatase | 4086 |
| 1Cu/$TiO_2$ (A) | Cu | 1 | 100% Anatase | 7972 |
| 0.1Ag/$TiO_2$ (A) | Ag | 0.1 | 100% Anatase | 997 |
| 0.25Ag/$TiO_2$ (A) | Ag | 0.25 | 100% Anatase | 2149 |
| 0.1Ag/$TiO_2$ (R) | Ag | 0.1 | 100% Rutile | 1002 |
| 0.25Ag/$TiO_2$ (R) | Ag | 0.25 | 100% Rutile | 2204 |
| 0.1Cu/$TiO_2$ (95 R) | Cu | 0.1 | 95% Rutile/5% Anatase | 1015 |
| 0.1Cu/$TiO_2$ (90 R) | Cu | 0.1 | 90% Rutile/10% Anatase | 1015 |
| 0.1Cu/$TiO_2$ (80 R) | Cu | 0.1 | 80% Rutile/20% Anatase | 1015 |
| 0.1Cu/$TiO_2$ (70 R) | Cu | 0.1 | 70% Rutile/30% Anatase | 1004 |
| 0.25Ag/$TiO_2$ (95 R) | Ag | 0.25 | 95% Rutile/5% Anatase | 1007 |
| 0.25Ag/$TiO_2$ (90 R) | Ag | 0.25 | 90% Rutile/10% Anatase | 1009 |
| 0.25Ag/$TiO_2$ (80 R) | Ag | 0.25 | 80% Rutile/20% Anatase | 1012 |
| 0.25Ag/$TiO_2$ (70 R) | Ag | 0.25 | 70% Rutile/30% Anatase | 1003 |

### 3.3. $N_2$ Absorption Studies

The porosity and the specific surface area are of high importance for materials used as substrates. For that purpose, the three different titania substrates and the samples 0.1Cu/$TiO_2$ (R), 0.25Cu/$TiO_2$ (R), 0.5Cu/$TiO_2$ (R), and 0.25Cu/$TiO_2$ (A) were subjected to $N_2$ physisorption tests at −195.850 °C. The Brunauer–Emmett–Teller (BET) method was used for the specific surface area, pore volume, and pore size determination, and Barrett, Joyner, and Halenda (BJH) absorption was used for pore distribution determination.

All the obtained isotherms were similar to the one that is described in Figure 5b. There are six types of isotherm curves according to the IUPAC classification: ones that are typical of microporous adsorbents (type I), nonporous or macroporous adsorbents (types II, III, and VI), or mesoporous adsorbents (types IV and V). According to that classification of the porous material isotherms [39,40], this type of isotherm has the same shape as type II isotherms (Figure 5a) that are complex in nature to obtain information about the pore morphology [41]. In this type of isotherms of combined micro-/mesoporous adsorbents, the interactions which are involved are due to the combination of adsorbent–adsorbate and adsorbate–adsorbate interactions.

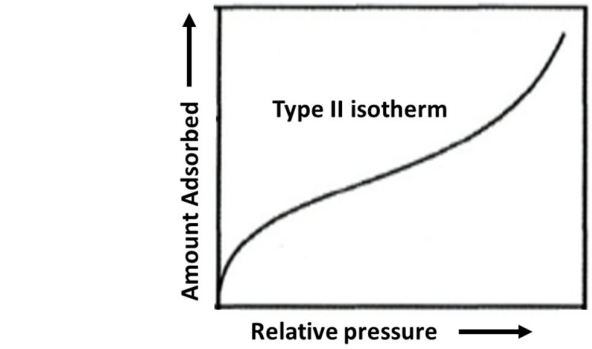


(**a**)

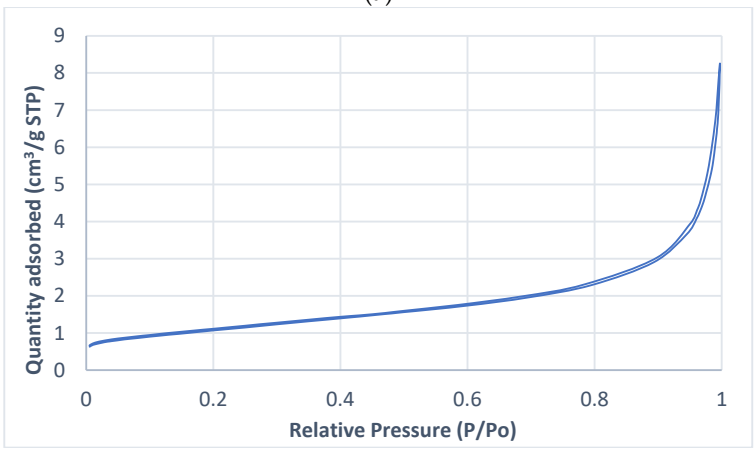


(**b**)

**Figure 5.** (**a**) Type II isotherm according to IUPAC (prepared according to [39]). And (**b**) Isotherm curve of sample 0.5Cu/$TiO_2$ (R).

The adsorption hysteresis curves are also empirically classified by IUPAC. It is widely accepted that there is a correlation between the shape of the hysteresis loop and the pore geometry of a mesoporous material. The hysteresis loop of our materials suggests the existence of cylindrical pores.

The specific surface area, the cumulative pore volume, and the pore size are summarized in Table 2 for all measured samples.

**Table 2.** Pore analysis characteristics.

| Sample Name | BET $m^2/g$ | BJH Adsorption Cumulative Pore Volume, $cm^3/g$ | Adsorption Average Pore Diameter, Å |
|---|---|---|---|
| $TiO_2$—Anatase | 9.93 | 0.025 | 127 |
| $TiO_2$—Rutile | 4.38 | 0.009 | 100 |
| 0.1Cu/$TiO_2$ (R) | 3.91 | 0.010 | 110 |
| 0.25Cu/$TiO_2$ (R) | 3.91 | 0.010 | 109 |
| 0.5Cu/$TiO_2$ (R) | 3.89 | 0.010 | 131 |
| 0.25Cu/$TiO_2$ (A) | 9.40 | 0.027 | 142 |

It appears that there are no major changes in the specific surface area (SSA) values of the derived photocatalysts, and these values are similar to their corresponding substrate. This can be attributed to the synthetic route that was employed and the small metal concentration in the resulting material. Titania rutile has the lowest SSA (4.38 $m^2/g$), while anatase exhibits the highest value (9.93 $m^2/g$). It is also observed that increasing the metal loading from 0.1 to 0.5 results in an increase in the average pore diameter.

### *3.4. Photocatalytic Studies*

With the use of these three types of titania substrates, various photocatalysts were synthesized to investigate and optimize the photocatalytic properties of the as-derived catalysts. The parameters that were examined are the copper loading effect on different substrates, the influence of silver loading on various substrates, the effect of catalyst concentration, and the rutile/anatase concentration ratio effect.

#### 3.4.1. Copper Loading Effect on Different Substrates

The effect of copper loading on titania rutile was investigated to determine the optimum copper loading on the latter substrate regarding the material's photocatalytic activity. Four different photocatalysts were prepared by changing the metal loading concentration on the substrate from 0.1 up to 1% *w*/*w*. Interestingly, 0.1 and 0.25% Cu-supported photocatalysts were found to be superior during the MB decolorization under visible light compared to pure $TiO_2$ (R). Cu loading of 0.1% appeared to be the most effective doping, as it achieved the highest degradation at 4 h under visible light. At 4 h irradiation, almost 100% (97%) MB decolorization was accomplished (Figure 6).

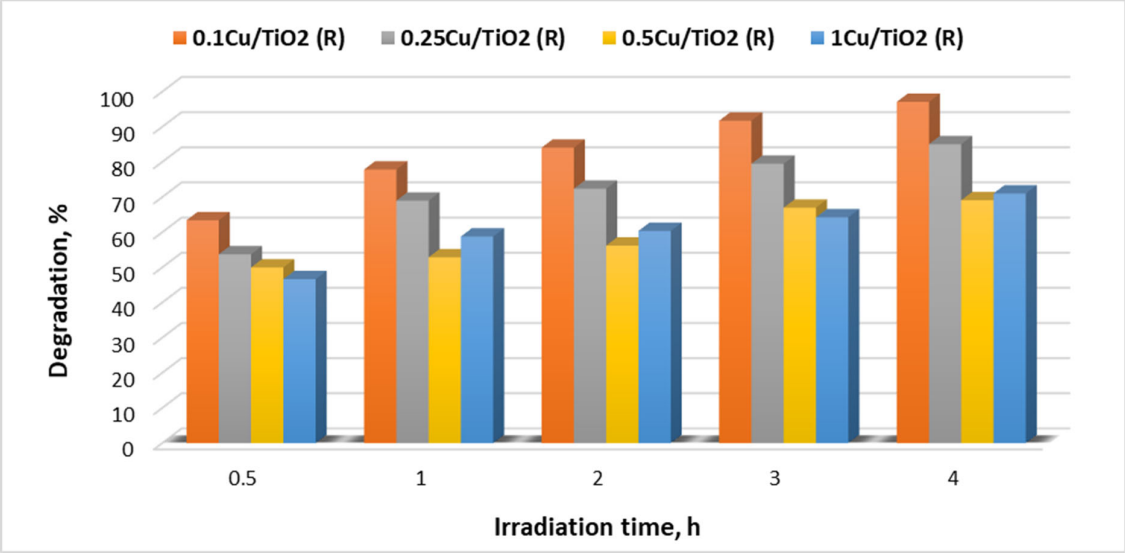


**Figure 6.** Cu loading concentration influence on photocatalytic activity under visible light.

Titania anatase was also tested as a substrate for the photocatalyst. Metal loadings of 0.1 and 0.25% copper were tested on anatase titania substrate. The results are presented in Figure 7. According to Figure 7, the increase in the irradiation time results in the MB concentration decreasing at a different rate depending on the time interval. The degradation reaction is much faster during the first hour of irradiation. Kinetics in heterogeneous catalysis is highly non-linear due to vastly different rates among elementary steps and competition for active sites among intermediates [42]. The obtained curves dictate that the catalysts prepared with titania anatase exhibited significantly lower photocatalytic activity towards the MB decolorization.

According to the latter findings, it is obvious that 0.1% Cu loading on rutile titania is the most suitable amongst the examined catalysts, as it possesses the highest activity under visible light.

Metal loading above 0.5% is not beneficial for either titania form. Possibly, the metal copper particles act as sites for the recombination of the generated electron holes and, hence, decrease the photocatalytic activity [43].

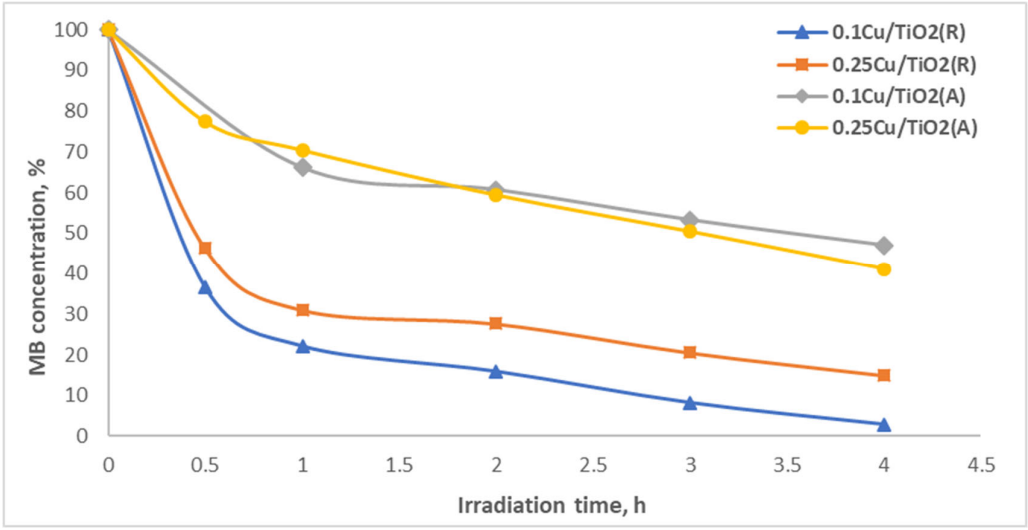


**Figure 7.** Influence of titania substrate nature (anatase or rutile) on Cu-doped catalysts' photocatalytic activity under visible light.

Likely, the Cu addition has opposite effects on the photocatalytic efficiency of $Cu/TiO_2$ catalysts. Thus, the catalytic activity of the samples is a synergistic effect of those parameters.

Titania rutile is a more efficient substrate for copper addition. Both the photocatalysts prepared with the same % metal loading but with rutile as substrate were significantly superior in terms of photocatalytic MB degradation. Titania anatase has a 3.2 eV energy band gap that is higher than that of the Rutile $TiO_2$ (3.0 eV) [44]. Since the metal addition further decreases the photocatalysts' energy band gap, it could possibly justify its enhanced efficiency towards the MB degradation under visible light.

### 3.4.2. Influence of Silver Loading on Various Substrates

The two optimum metal concentrations (0.1% and 0.25%), based on the copper results in Section 3.4.1, were also used for the synthesis of silver-doped titania photocatalysts. The $Ag/TiO_2$ photocatalysts were examined towards MB degradation. It is suggested that the silver loading was beneficial for $TiO_2$ rutile. Both metal loadings exhibited good catalytic activity under visible light, as demonstrated in Figure 8.

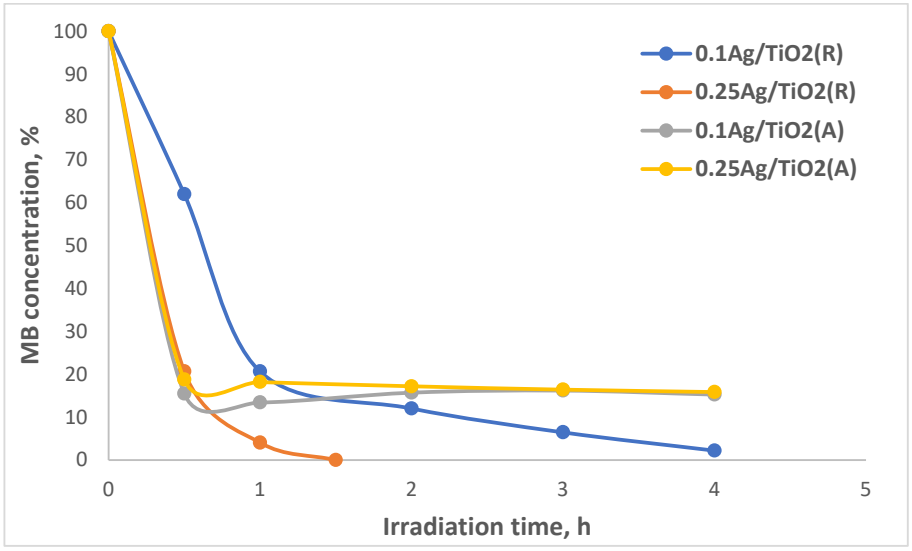


**Figure 8.** Influence of titania substrate nature on Ag-doped catalysts' photocatalytic activity under visible light.

The 0.25% silver-supported rutile catalyst exhibited the highest catalytic performance among the tested ones under visible light. The titania rutile seemed to act more efficiently as a substrate for metal loading, as their combination exhibited the optimum photocatalytic performance under visible light. This point is also supported by the Cu-$TiO_2$ experiment series.

### 3.4.3. Effect of Catalyst Concentration

The influence of the photocatalyst concentration in the MB solution was studied. The most active catalyst (0.25Ag/$TiO_2$ (R)) was employed for the determination of the optimum concentration value. The tested concentrations varied from 3 to 6 g/L (grams per liter MB solution), and the as-derived photocatalytic results are presented in Figure 9.

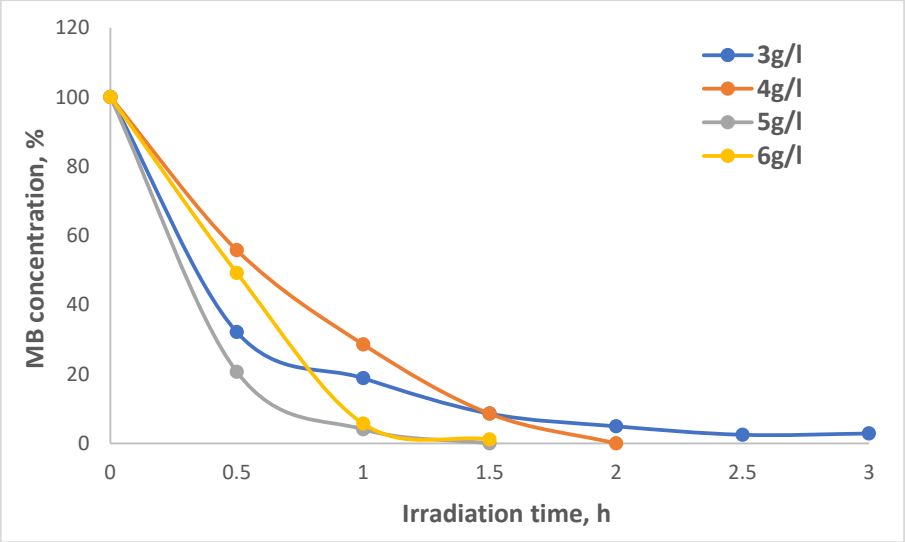


**Figure 9.** Effect of catalyst concentration on catalytic behavior towards the MB degradation under visible light.

The optimum concentration appeared to be 5 g/L since the catalyst achieved 100% MB degradation in the shortest time (1.5 h). An increase in the catalyst concentration above 5 g/L slightly deteriorated the degradation rate. This may be attributed to the shielding effect, where the high concentration of the particles in the solutions hinders the light fraction from being converted for electron excitation [45].

### 3.4.4. Rutile/Anatase Concentration Ratio Effect

To investigate the role of rutile content in the photocatalytic activity of our meta-doped titania, five different catalysts were synthesized by only changing the ratios between titania's forms—rutile and anatase. In each experiment, the 100% substrate was completed by summing the rutile and anatase percentage, e.g., in the experiment with 70% rutile content, the other 30% is titania anatase. Their photocatalytic activity was evaluated towards the MB decolorization under UV and visible light emission. Two different metal dopants—Cu and Ag—were investigated, and the acquired results are presented in Figure 10. The optimum metal concentrations were chosen for each metal for a higher evaluation degree of the resulting photocatalyst.

The results indicated that the ratio 95% rutile–5% anatase is the most beneficial substrate for both metal dopants towards the examined photocatalytic reaction. More specifically, in the case of Cu-based photocatalyst, the catalyst prepared with 5% anatase and 95% rutile achieved a major decrease in the irradiation time required to achieve 90% MB degradation (from 2.5 h to 1 h), comparing the results of Figures 7 and 10.

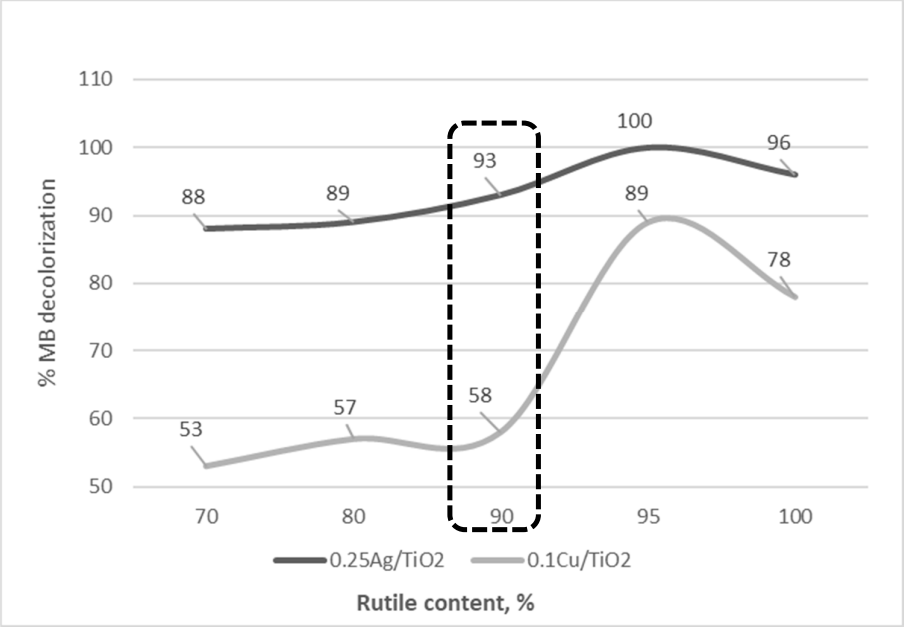


**Figure 10.** Rutile content effect on Ag- and Co-doped photocatalysts after 1 h of irradiation.

The results suggest that the introduction of a small quantity of anatase titania (5%) considerably increases the activity of the examined photocatalysts towards methylene blue degradation. It was previously reported that the remarkable co-existent effect of rutile and anatase would arise from the increase in the charge separation efficiency due to photoinduced interfacial electron transfer from anatase to rutile under UV light excitation. In this study, the preferential Ag deposition on the anatase/rutile interface was held responsible for the superior photocatalytic activity in the case of the anatase and rutile mix substrate [46]. There are previous studies that demonstrate the photocatalytic superiority of catalysts prepared with a mixture of titania phases compared to those prepared with pure anatase or pure rutile. These data strongly indicate the existence of a synergistic effect between anatase and rutile phases in the metal-doped photocatalyst under visible light excitation. This synergistic phenomenon is similar to that of $TiO_2$ under UV light excitation. In their approach, though, the Sm-doped titania photocatalysts were prepared via a sol-gel approach using precursor compounds for the metal and the titania synthesis [47].

## 4. Conclusions

The one-step preparation approach that was followed successfully provided photocatalysts that were proved to be highly active under visible light irradiation towards the methylene blue degradation reaction. The experimental results suggested that titania rutile is a better substrate for the catalyst, compared to titania anatase for the wet impregnation PROMETHEUS synthesis approach followed in this study.

It is determined that 0.1% Cu and 0.25% Ag loading on 95% rutile–5% anatase titania are the optimum amongst the examined catalysts, as it possesses the highest activity under visible light. The results indicated that the ratio 95% rutile–5% anatase is the most beneficial substrate for both metal dopants towards the examined photocatalytic reaction. More specifically, in the case of the Cu-based photocatalyst, the catalyst prepared with 5% anatase and 95% rutile achieved a major decrease of more than 50% (from 4 h irradiation to 1 h 45 min) for the required irradiation time to accomplish 100% MB degradation.

Furthermore, it is established that metal loading equal to or above 0.5% is not beneficial for either titania form. It is assumed that the metal copper particles act as sites for the recombination of the generated electron holes and, hence, decrease the photocatalytic activity. Further studies on this matter will be beneficial to confirm this hypothesis. Photoluminescence studies on the produced photocatalysts, as well as measurements of UV–Vis

diffuse reflectance spectra of the photocatalysts for the determination of their energy band gap, will provide more data to further elaborate this finding.

**Author Contributions:** Conceptualization, K.M.S. and I.Y.; methodology, A.M.M., E.P. and O.T.; software, O.T.; validation, A.M.M., K.M.S. and I.Y.; formal analysis, O.T. and A.M.M.; investigation, O.T.; data curation, O.T. and A.M.M.; writing—original draft preparation, O.T. and A.M.M.; writing—review and editing, A.M.M., K.M.S., E.P. and I.Y.; visualization, A.M.M., K.M.S. and I.Y.; supervision, E.P. and I.Y. All authors have read and agreed to the published version of the manuscript.

**Funding:** Part of this investigation was co-funded by the European Regional Development Fund and the Republic of Cyprus for the "RESTART 2016–2020" Programmes for Research, Technological Development and Innovation (RTDI) within the framework of the research project PHOTO_COVID: Photocatalytic coating for the reduction of the COVID outbreak. (RPF Proposal Number: SEED-COVID/0420/0031).

**Institutional Review Board Statement:** Not applicable.

**Informed Consent Statement:** Not applicable.

**Data Availability Statement:** Data is contained within the article.

**Conflicts of Interest:** The authors declare no conflict of interest.

## References

1. Hassanpour, M.; Safardoust-Hojaghan, H.; Salavati-Niasari, M. Degradation of Methylene Blue and Rhodamine B as Water Pollutants via Green Synthesized $Co_3O_4$/ZnO Nanocomposite. *J. Mol. Liq.* **2017**, *229*, 293–299. [CrossRef]
2. Chakhtouna, H.; Benzeid, H.; Zari, N.; Qaiss, A.E.K.; Bouhfid, R. Recent Progress on Ag/$TiO_2$ Photocatalysts: Photocatalytic and Bactericidal Behaviors. *Environ. Sci. Pollut. Res. Int.* **2021**, *28*, 44638–44666. [CrossRef] [PubMed]
3. Duan, Z.; Huang, Y.; Zhang, D.; Chen, S. Electrospinning Fabricating Au/$TiO_2$ Network-like Nanofibers as Visible Light Activated Photocatalyst. *Sci. Rep.* **2019**, *9*, 8008. [CrossRef] [PubMed]
4. Etacheri, V.; Di Valentin, C.; Schneider, J.; Bahnemann, D.; Pillai, S.C. Visible-Light Activation of $TiO_2$ Photocatalysts: Advances in Theory and Experiments. *J. Photochem. Photobiol. C Photochem. Rev.* **2015**, *25*, 1–29. [CrossRef]
5. Xu, C.; Rangaiah, G.P.; Zhao, X.S. Photocatalytic Degradation of Methylene Blue by Titanium Dioxide: Experimental and Modeling Study. *Ind. Eng. Chem. Res.* **2014**, *53*, 14641–14649. [CrossRef]
6. Chauhan, R.; Kumar, A.; Pal Chaudhary, R. Photocatalytic Degradation of Methylene Blue with Cu Doped ZnS Nanoparticles. *J. Lumin.* **2014**, *145*, 6–12. [CrossRef]
7. Reza, K.M.; Kurny, A.; Gulshan, F. Photocatalytic Degradation of Methylene Blue by Magnetite+$H_2O_2$+UV Process. *Int. J. Environ. Sci. Dev.* **2016**, *7*, 325–329. [CrossRef]
8. Jing, H.-P.; Wang, C.-C.; Zhang, Y.-W.; Wang, P.; Li, R. Photocatalytic Degradation of Methylene Blue in ZIF-8. *RSC Adv.* **2014**, *4*, 54454–54462. [CrossRef]
9. Trandafilović, L.V.; Jovanović, D.J.; Zhang, X.; Ptasińska, S.; Dramićanin, M.D. Enhanced Photocatalytic Degradation of Methylene Blue and Methyl Orange by ZnO:Eu Nanoparticles. *Appl. Catal. B* **2017**, *203*, 740–752. [CrossRef]
10. Lin, J.; Luo, Z.; Liu, J.; Li, P. Photocatalytic Degradation of Methylene Blue in Aqueous Solution by Using ZnO-$SnO_2$ Nanocomposites. *Mater. Sci. Semicond. Process.* **2018**, *87*, 24–31. [CrossRef]
11. Pirbazari, A.E.; Monazzam, P.; Kisomi, B.F. Co/$TiO_2$ Nanoparticles: Preparation, Characterization and Its Application for Photocatalytic Degradation of Methylene Blue. *Desalin Water Treat* **2017**, *63*, 283–292. [CrossRef]
12. Yang, Y.; Xu, L.; Wang, H.; Wang, W.; Zhang, L. $TiO_2$/Graphene Porous Composite and Its Photocatalytic Degradation of Methylene Blue. *Mater. Des.* **2016**, *108*, 632–639. [CrossRef]
13. Lu, K.-Q.; Li, Y.-H.; Tang, Z.-R.; Xu, Y.-J. Roles of Graphene Oxide in Heterogeneous Photocatalysis. *ACS Mater. Au* **2021**, *1*, 37–54. [CrossRef]
14. Khalil, M.; Anggraeni, E.S.; Ivandini, T.A.; Budianto, E. Exposing $TiO_2$ (001) Crystal Facet in Nano Au-$TiO_2$ Heterostructures for Enhanced Photodegradation of Methylene Blue. *Appl. Surf. Sci.* **2019**, *487*, 1376–1384. [CrossRef]
15. Lv, T.; Zhao, J.; Chen, M.; Shen, K.; Zhang, D.; Zhang, J.; Zhang, G.; Liu, Q. Boosted Visible-Light Photodegradation of Methylene Blue by V and Co Co-Doped $TiO_2$. *Materials* **2018**, *11*, 1946. [CrossRef]
16. Murcia Mesa, J.J.; Guarín Romero, J.R.; Cely Macías, Á.C.; Rojas Sarmiento, H.A.; Cubillos Lobo, J.A.; Navío Santos, J.A.; Hidalgo López, M.D.C. Methylene Blue Degradation over M-$TiO_2$ Photocatalysts (M = Au or Pt)/Degradación de Azul de Metileno Sobre Fotocatalizadores M-$TiO_2$ (M = Au o Pt). *Cienc. Desarro.* **2017**, *8*, 109–117. [CrossRef]
17. Anwar, D.I.; Mulyadi, D. Synthesis of Fe-$TiO_2$ Composite as a Photocatalyst for Degradation of Methylene Blue. *Procedia Chem.* **2015**, *17*, 49–54. [CrossRef]

18. Tariq, M.K.; Riaz, A.; Khan, R.; Wajid, A.; Haq, H.-U.; Javed, S.; Akram, M.A.; Islam, M. Comparative Study of Ag, Sn or Zn Doped $TiO_2$ Thin Films for Photocatalytic Degradation of Methylene Blue and Methyl Orange. *Mater. Res. Express* **2019**, *6*, 106435. [CrossRef]
19. Orlandi, M.; Dalle Carbonare, N.; Caramori, S.; Bignozzi, C.A.; Berardi, S.; Mazzi, A.; Koura, Z.E.; Bazzanella, N.; Patel, N.; Miotello, A. Porous versus Compact Nanosized Fe(III)-Based Water Oxidation Catalyst for Photoanodes Functionalization. *ACS Appl. Mater. Interf.* **2016**, *8*, 20003–20011. [CrossRef]
20. Koura, Z.E.; Rossi, G.; Calizzi, M.; Amidani, L.; Pasquini, L.; Miotello, A.; Boscherini, F. XANES study of vanadium and nitrogen dopants in photocatalytic $TiO_2$ thin films. *Phys. Chem. Chem. Phys.* **2018**, *20*, 221–231. [CrossRef]
21. Koura, Z.E.; Patel, N.; Edla, R.; Miotello, A. Multilayer films of indium tin oxide/$TiO_2$ codoped with vanadium and nitrogen for efficient photocatalytic water splitting. *Int. J. Nanotechnol.* **2014**, *11*, 1017. [CrossRef]
22. Alkaykh, S.; Mbarek, A.; Ali-Shattle, E.E. Photocatalytic Degradation of Methylene Blue Dye in Aqueous Solution by $MnTiO_3$ Nanoparticles under Sunlight Irradiation. *Heliyon* **2020**, *6*, e03663. [CrossRef] [PubMed]
23. Rather, R.A.; Singh, S.; Pal, B. Photocatalytic Degradation of Methylene Blue by Plasmonic Metal-$TiO_2$ Nanocatalysts under Visible Light Irradiation. *J. Nanosci. Nanotechnol.* **2017**, *17*, 1210–1216. [CrossRef] [PubMed]
24. Gao, F.; Jiang, J.; Du, L.; Liu, X.; Ding, Y. Stable and Highly Efficient Cu/$TiO_2$ Nanocomposite Photocatalyst Prepared through Atomic Layer Deposition. *Appl. Catal. A Gen.* **2018**, *568*, 168–175. [CrossRef]
25. Khannyra, S.; Mosquera, M.J.; Addou, M.; Gil, M.L.A. Cu-$TiO_2$/$SiO_2$ Photocatalysts for Concrete-Based Building Materials: Self-Cleaning and Air de-Pollution Performance. *Constr. Build. Mater.* **2021**, *313*, 125419. [CrossRef]
26. De Los Santos, D.M.; Chahid, S.; Alcántara, R.; Navas, J.; Aguilar, T.; Gallardo, J.J.; Gómez-Villarejo, R.; Carrillo-Berdugo, I.; Fernández-Lorenzo, C. $MoS_2$/Cu/$TiO_2$ Nanoparticles: Synthesis, Characterization and Effect on Photocatalytic Decomposition of Methylene Blue in Water under Visible Light. *Water Sci. Technol.* **2018**, *2017*, 184–193. [CrossRef]
27. Wang, M.; Peng, L.; Wang, J.; Li, C.; Guan, L.; Lin, Y. Enhanced Visible Light Photocatalytic Decolorization of Methylene Blue by Hierarchical Ternary Nanocomposites Cu-$TiO_2$-Mesoporous-Silica Microsphere. *J. Nanosci. Nanotechnol.* **2018**, *18*, 8269–8275. [CrossRef]
28. Koura, Z.E.; Cazzanelli, M.; Bazzanella, N.; Patel, N.; Fernandes, R.; Arnaoutakis, G.E.; Gakamsky, A.; Dick, A.; Quaranta, A.; Miotello, A. Synthesis and Characterization of Cu and N Codoped RF-Sputtered $TiO_2$ Films: Photoluminescence Dynamics of Charge Carriers Relevant for Water Splitting. *J. Phys. Chem. C* **2016**, *120*, 12042–12050. [CrossRef]
29. Jaiswal, R.; Bharambe, J.; Patel, N.; Dashora, A.; Kothari, D.C.; Miotello, A. Copper and Nitrogen co-doped $TiO_2$ photocatalyst with enhanced optical absorption and catalytic activity. *Appl. Catal. B* **2015**, *168–169*, 333–341. [CrossRef]
30. Skiba, M.; Vorobyova, V. Synthesis of AG/$TIO_2$ Nanocomposite via Plasma Liquid Interactions and Degradation Methylene Blue. *Appl. Nanosci.* **2020**, *10*, 4717–4723. [CrossRef]
31. Singh, J.; Tripathi, N.; Mohapatra, S. Synthesis of Ag–$TiO_2$ Hybrid Nanoparticles with Enhanced Photocatalytic Activity by a Facile Wet Chemical Method. *Nano-Struct. Nano-Objects* **2019**, *18*, 100266. [CrossRef]
32. Díaz-Uribe, C.; Viloria, J.; Cervantes, L.; Vallejo, W.; Navarro, K.; Romero, E.; Quiñones, C. Photocatalytic Activity of Ag-$TiO_2$ Composites Deposited by Photoreduction under UV Irradiation. *Int. J. Photoenergy* **2018**, *2018*, 6080432. [CrossRef]
33. Bhardwaj, S.; Pal, B. Photodeposition of Ag and Cu Binary Co-Catalyst onto $TiO_2$ for Improved Optical and Photocatalytic Degradation Properties. *Adv. Powder Technol.* **2018**, *29*, 2119–2128. [CrossRef]
34. Xie, L.; Hao, J.-G.; Chen, H.-Q.; Li, Z.-X.; Ge, S.-Y.; Mi, Y.; Yang, K.; Lu, K.-Q. Recent advances of nickel hydroxide-based cocatalysts in heterogeneous photocatalysis. *Catal. Commun.* **2022**, *162*, 106371. [CrossRef]
35. Chen, H.-Q.; Hao, J.-G.; Wei, Y.; Huang, W.-Y.; Zhang, J.-L.; Deng, T.; Yang, K.; Lu, K.-Q. Recent Developments and Perspectives of Cobalt Sulfide-Based Composite Materials in Photocatalysis. *Catalysts* **2023**, *13*, 544. [CrossRef]
36. Yakoumis, I. PROMETHEUS: A Copper-Based Polymetallic Catalyst for Automotive Applications. Part I: Synthesis and Characterization. *Materials* **2021**, *14*, 622.
37. Yakoumis, I. Copper and Noble Metal Polymetallic Catalysts for Engine Exhaust Gas Treatment. European Patent EP3569309, 20 November 2019.
38. Ijadpanah-Saravy, H.; Safari, M.; Khodadadi-Darban, A.; Rezaei, A. Synthesis of Titanium Dioxide Nanoparticles for Photocatalytic Degradation of Cyanide in Wastewater. *Anal.Lett.* **2014**, *47*, 1772–1782. [CrossRef]
39. Sing, K.S.W.; Everett, D.H.; Haul, R.A.W.; Moscou, L.; Pierotti, R.A.; Rouquerol, J.; Siemieniewska, T. Reporting physisorption data for gas/solid systems with special reference to the determination of surface area and porosity. *Pure Appl. Chem.* **1985**, *57*, 603–619. [CrossRef]
40. Broekhoff, J.C.P. Mesopore determination from nitrogen sorption isotherms: Fundamentals, scope, limitations. In *Studies in Surface Science and Catalysis*; Elsevier: Amsterdam, The Netherlands, 1979; Volume 3, pp. 663–684.
41. Kumar, K.V.; Gadipelli, S.; Wood, B.; Ramisetty, K.A.; Stewart, A.A.; Howard, C.A.; Brett, D.J.B.; Rodriguez-Reinoso, F. Characterization of adsorption site energies and heterogeneous surfaces of porous materials. *J. Mater. Chem. A* **2019**, *7*, 10104–10137. [CrossRef]
42. Bouras, P.; Stathatos, E.; Lianos, P. Pure versus metal-ion-doped nanocrystalline titania for photocatalysis. *Appl. Catal. B* **2007**, *73*, 51–59. [CrossRef]
43. Lynggaard, H.; Andreasen, A.; Stegelmann, C.; Stoltze, P. Analysis of simple kinetic models in heterogeneous catalysis. *Prog. Surf. Sci.* **2004**, *77*, 71–137. [CrossRef]

44. Xia, X.H.; Gao, Y.; Wang, Z.; Jia, Z.J. Structure and photocatalytic properties of copper-doped rutile $TiO_2$ prepared by a low-temperature process. *J. Phys. Chem. Solids* **2008**, *69*, 2888–2893. [CrossRef]
45. Tichapondwa, S.M.; Newman, J.P.; Kubhek, O. Effect of $TiO_2$ phase on the photocatalytic degradation of methylene blue dye. *Phys. Chem. Earth Parts A/B/C* **2020**, *118–119*, 102900. [CrossRef]
46. Miyagi, T.; Kamei, M.; Mitsuhashi, T.; Ishigaki, T.; Yamazaki, A. Charge separation at the rutile/anatase interface: A dominant factor of photocatalytic activity. *Chem. Phys. Lett.* **2004**, *390*, 399–402. [CrossRef]
47. Xiao, Q.; Si, Z.; Yu, Z.; Qiu, G. Sol–gel auto-combustion synthesis of samarium-doped $TiO_2$ nanoparticles and their photocatalytic activity under visible light irradiation. *MSEB* **2007**, *137*, 189–194. [CrossRef]